Observation of cyclotron antiresonance in the topological insulator Bi_{2}Te_{3}

S. V. Dordevic, Hechang Lei, C. Petrovic, J. Ludwig, Z. Q. Li, and D. Smirnov

Phys. Rev. B **98**, 115138 — Published 20 September 2018

DOI: 10.1103/PhysRevB.98.115138

Observation of cyclotron anti-resonance in topological insulator Bi_2Te_3

S.V. Dordevic
Department of Physics, The University of Akron, Akron, Ohio 44325 USA

Hechang Lei* and C. Petrovic
Condensed Matter Physics and Materials Science Department, Brookhaven National Laboratory, Upton, New York 11973 USA

J. Ludwig, Z.Q. Li†, and D. Smirnov
National High Magnetic Field Laboratory, Tallahassee, Florida 32310 USA

(Dated: August 9, 2018)

We report on the experimental observation of a cyclotron anti-resonance in a canonical 3D topological insulator Bi_2Te_3. Magneto-reflectance response of single crystal Bi_2Te_3 was studied in 18 Tesla magnetic field, and compared to other topological insulators studied before, the main spectral feature is inverted. We refer to it as an anti-resonance. In order to describe this unconventional behaviour we propose the idea of an imaginary cyclotron resonance frequency, which on the other hand indicates that the form of the Lorentz force that magnetic field exerts on charge carriers takes an unconventional form.

PACS numbers: 78.20.Ci, 78.30.-j, 74.25.Gz

For decades cyclotron resonance has been an important experimental tool in plasma[1–3] and condensed matter physics[4,5]. In condensed matter physics for example, cyclotron resonance has been used for probing charge dynamics, in particular in semiconductors. Valuable information about band structure, carrier scattering rate, effective mass, etc. can be obtained from these measurements. In recent years, with the advent of materials with Dirac electrons like graphene and topological insulators, cyclotron resonance measurements have been extensively used for probing their electronic structure. Cyclotron resonance has been observed and characterized in single and multiple layer graphene[6], thin films of Bi_2Se_3[7], bulk Bi_2Se_3[8], elemental bismuth[9–11], $Bi_{1-x}Sb_x$[12,13], $Bi_{1-x}As_x$[14], $(Bi_{1-x}Sb_x)_2Te_3$[15], nano-flakes of Bi_2Te_3[16], etc.

In this work we used magneto-optical spectroscopy to study topological insulator Bi_2Te_3. Magneto-optical activity was detected in reflection spectra, but surprisingly in Bi_2Te_3 we observed cyclotron *anti-resonance*, where the spectral feature is inverted, i.e. it is a mirror image of the resonance observed in other systems. For comparison we also measured another canonical topological insulator from the same family Sb_2Te_3, and we observed a conventional resonance. Based on our data analysis we suggest that the anti-resonance in Bi_2Te_3 is due to an unconventional form of the Lorentz force that external magnetic exerts on the charge carriers.

Single crystals of Bi_2Te_3 and Sb_2Te_3 were grown at Brookhaven National Laboratory[17,18] and characterized with X-ray diffraction using a Rigaku Miniflex X-ray machine. The analysis showed that samples were single phase, and with lattice parameters consistent with the previously published values[19]. Samples had a thickness of several millimeters, and naturally flat surfaces with a typical size of about 3 mm. Before every spectroscopic measurement the samples were mechanically cleaved in order to expose a fresh surface.

Far-infrared and mid-infrared magneto-reflectance ratios R(ω,B)/R(ω, 0 T) were collected at the National High Magnetic Field Laboratory using superconducting 18 T magnet. Reflectance ratios provide the most direct evidence for magneto-optical activity, as they do not require any data analysis or manipulation. All measurements were performed at 5 K, with unpolarized light and with the electric field vector parallel to the quintuple layers of Bi_2Te_3 and Sb_2Te_3, i.e. in Faraday geometry.

Figure 1 shows the infrared reflectance ratios R(ω, B)/R(ω, 0 T) of Bi_2Te_3 and Sb_2Te_3 in magnetic fields up to 18 T. In Bi_2Te_3 we observed magnetic field induced changes in reflectance (Fig. 1(a)), exceeding 20 % in 18 T, in the region around 800 cm^{-1} (100 meV). This is precisely the region where the plasma minimum was observed in the zero-field reflectance[20]. In Fig. 1(b) we display the ratios for Sb_2Te_3 and they also show field induced changes with the maximum change of about 10 % around 1,300 cm^{-1} (160 meV), which is the location of plasma minimum in zero field reflectance[20]. In Sb_2Te_3 conventional cyclotron resonance is observed, similar to other systems, such as graphene, Bi_2Se_3, bismuth, $Bi_{1-x}Sb_x$, etc. The resonance in these systems manifest as a characteristic dip-peak structure in reflectance ratios. Contrary to all of them, in Bi_2Te_3 we observe the exactly opposite: a peak-dip structure, and we refer to it as an anti-resonance[21].

In other to explore the origins of observed cyclotron anti-resonance we employ Drude model modified for the presence of magnetic field[22]. In spite of its simplicity, this model has been very successful in describing magneto-optical data in a variety of condensed matter systems, most notably topological insulators[8,9,13,23]. In the semi-

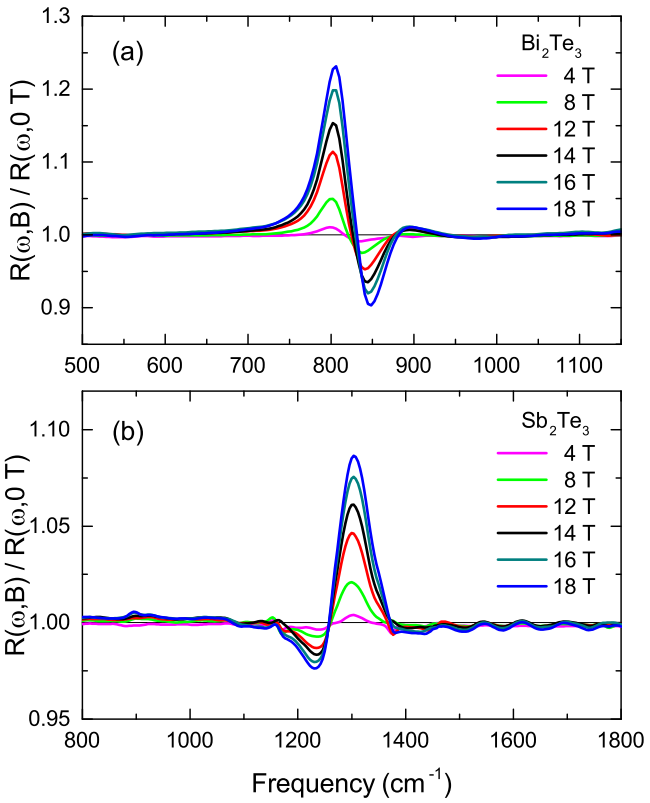

FIG. 1: (Color online). (a) Reflection ratios of Bi_2Te_3 at several magnetic field values. The feature around 800 cm^{-1} is identified as cyclotron anti-resonance, because it is a mirror image of the feature observed in Sb_2Te_3 (bottom panel). (b) Reflection ratios of Sb_2Te_3 at several magnetic field values. The feature around 1,300 cm^{-1} is identified as the usual cyclotron resonance. Note different axes scales between the two panels.

classical approximation, the dynamics of charge carriers (with effective mass m) in a solid is governed by[24]:

$$m\frac{d\vec{v}}{dt} + m\gamma\vec{v} = -e\vec{E} - e\vec{v}\times\vec{B_0} \qquad (1)$$

where the expression on the right is the Lorentz force, with constant magnetic field B_0 being applied along z-axis. Assuming that both $\vec{v}$ and $\vec{E}$ vary as $e^{-i\omega t}$, one can solve[24] for the complex dielectric function for the left and right circularly polarized light $\tilde{\varepsilon}_{\pm}(\omega)$ as:

$$\tilde{\varepsilon}_{\pm}(\omega) = \varepsilon_{\infty} + \frac{\omega_p^2}{-\omega^2 - i\gamma\omega \mp \omega_c\omega} \qquad (2)$$

where ω_p is the oscillator strength of the resonance mode and γ is its width. ε_{∞} is the high-frequency dielectric constant. $\omega_c = eB_0/m$ is the cyclotron resonance frequency, and is conventionally taken as positive for electron-like and negative for hole-like carriers. Using this model we could obtain good fits of reflectance ratios of Sb_2Te_3. In Sb_2Te_3 (and Bi_2Te_3) charge carriers are believed to be hole-like[20], so ω_c is taken as negative. The best fits are shown in Fig. 2(b) with black lines. We notice that the model is capable of capturing all the important features of Sb_2Te_3 data, in particular, the dip-peak structure characteristic of cyclotron resonance seen in other systems, such as Bi_2Se_3[8].

On the other hand, we have not been able to obtain satisfactory fits of reflectance ratios of Bi_2Te_3 for any values of model parameters. In particular, the model cannot reproduce the peak-dip structure characteristic of Bi_2Te_3 data. To circumvent this problem we propose the idea that in Bi_2Te_3 cyclotron resonance frequency acquires imaginary (or more generally complex) values. Imaginary cyclotron resonance frequency is necessary in order to introduce an additional phase shift in the dielectric function (Eq. 2). The idea was inspired by the recently proposed theory to explain quantum fluctuating superconductivity[27]. The authors used a complex cyclotron frequency, and referred to it as the super-cyclotron resonance.

Cyclotron resonance is a direct consequence of applied magnetic field (Eq. 1) and therefore in order to obtain imaginary cyclotron frequency, one must modify the expression for the Lorentz force that magnetic field exerts on charge carriers. We propose that in the case of Bi_2Te_3 the magnetic part of the Lorentz force should be modified to:

$$\vec{F} = -e\frac{1}{\gamma}\frac{d\vec{v}}{dt}\times\vec{B_0}. \qquad (3)$$

Other, more complicated modifications to the Lorentz force are also possible. Making the same assumptions as before[24], and solving in the semi-classical approximation as before (Eq. 1), one obtains for the complex dielectric function:

$$\tilde{\varepsilon}_{\pm}(\omega) = \varepsilon_{\infty} + \frac{\omega_p^2}{-\omega^2 - i\gamma\omega \mp i\omega^2\omega_c'/\gamma} \qquad (4)$$

which, compared with Eq. 2, effectively has an imaginary cyclotron resonance frequency ω_c'. We note however, that the physical meaning of ω_c' is different from ω_c (from Eq. 2) and the two should not be directly compared. We also point out that Eq. 4 satisfies the causality relations $\tilde{\varepsilon}_{\pm}(-\omega) = \tilde{\varepsilon}^*_{\mp}(\omega)$.

Using this model (Eq. 4) we were able to obtain satisfactory fits for Bi_2Te_3. The results of the fits are shown with black lines in Fig. 2, for several magnetic field values. As can be seen, the fits can capture all the essential features of the data, in particular the peak-dip structure of Bi_2Te_3. We find this to be significant, as the conventional model (Eq. 2) cannot fit the data for any values of fitting parameters. It should also be noted that, even though the model Eq. 4 captures the most important feature of the data, it does not reproduce the data around

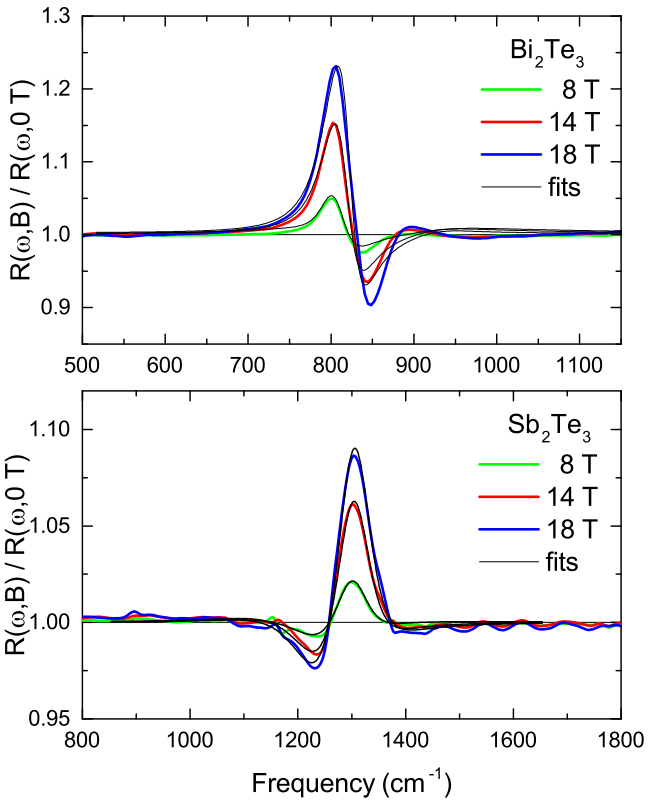

FIG. 2: (Color online). (a) The best fits of reflectance ratios of Bi_2Te_3 at several selected field values, using Eq. 4. (b) The best fits of reflectance ratios of Sb_2Te_3 at several selected field values, using Eq. 2.

900 cm^{-1}. This secondary, much weaker structure might be due to Landau level transitions, and additional terms might be needed in Eq. 4 to account for it.

In order to get a better insight into carrier dynamics, we explored other optical functions of both Bi_2Te_3 and Sb_2Te_3. From the best fits of reflectance obtained with Eqs. 2 and 4 we generated optical conductivities for left and right circular polarizations of light $\sigma_{\pm}(\omega) = \omega(\varepsilon_{\pm}(\omega)-1)/(4\pi i)$. Fig. 3 displays the real part of circular conductivity for both Bi_2Te_3 (top panels) and Sb_2Te_3 (bottom panels). For Sb_2Te_3 in zero field both $\sigma_-(\omega)$ and $\sigma_+(\omega)$ are Drude modes. As the field increases, $\sigma_+(\omega)$ is gradually suppressed, but maintains its Drude shape. On the other hand, the peak in $\sigma_-(\omega)$ is shifted to finite frequencies, and is gradually suppressed, but appears to maintain its width. At 18 T, the peak is at approximately 45 cm^{-1}. This behaviour is typical of topological insulators, and has been seen before, for example in Bi_2Se_3[7,8].

Surprisingly, the behaviour of both $\sigma_-(\omega)$ and $\sigma_+(\omega)$ (Fig. 3(a) and (b) respectively) in Bi_2Te_3 is similar to Sb_2Te_3, Bi_2Se_3 and other topological insulators. Even though the model used to fit the data was different, all the features in the $\sigma_{\pm}(\omega)$ spectra are qualitatively similar. In zero field both $\sigma_+(\omega)$ and $\sigma_-(\omega)$ are Drude modes. As the field increases, $\sigma_+(\omega)$ is suppressed, whereas in $\sigma_-(\omega)$ the peak gradually shifts to finite frequencies and at 18 T it is at 24 cm^{-1}.

In Fig. 4 we plot the parameters of the best fits from Eqs. 2 and 4. Fig. 4(a) and (b) display the cyclotron resonance frequencies ω_c' and ω_c for Bi_2Te_3 and Sb_2Te_3 respectively. In both compounds we observe linear field dependence which extrapolates to zero in zero field, characteristic of charge carriers with parabolic band dispersion. Linear fits (shown with dashed lines) yield $\hbar\omega_c/B$ = 0.025 meV/T and 0.27 meV/T for Bi_2Te_3 and Sb_2Te_3 respectively. In the case of Sb_2Te_3 we can estimate the cyclotron effective mass m/m_e = 0.42. This value is in general agreement with earlier reports from quantum oscillations measurements[25,26].

In summary, magneto-optical study of Bi_2Te_3 and Sb_2Te_3 has reveal a cyclotron resonance in the spectra of Sb_2Te_3, and an anti-resonance in Bi_2Te_3. To explain the behaviour of Bi_2Te_3 we introduced the idea of an alternative Lorentz force, which resulted in an imaginary cyclotron frequency. Physical interpretation of this unconventional behaviour requires deeper theoretical analysis of how light couples to charge carriers in Bi_2Te_3.

The authors thank A.B. Kuzmenko, Y. Zhang and X.R. Wang for useful discussions. Work at Brookhaven is supported by the US DOE under Contract No. DE-SC00112704 (H.L. and C.P.). A portion of this work was performed at the National High Magnetic Field Laboratory, which is supported by National Science Foundation Cooperative Agreement No. DMR-1157490 and the State of Florida.

* Present address: Department of Physics, Renmin University, Beijing 100872, China

† Present address: College of Physical Science and Technology, Sichuan University, Chengdu, 610064, China

/clearpage

[1] H. Hartmann and K.-P. Wanczek, *Ion Cyclotron Resonance Spectrometry*, Springer (1978).

[2] G. Guest, *Electron Cyclotron Heating of Plasmas*, Wiley-VCH, (2009).

[3] D.G. Lominadze, *Cyclotron Waves in Plasma*, Pergamon (2013).

[4] P.Y. Yu and M. Cardona, *Fundamentals of Semiconductors*, Springer (2010).

[5] S. Bhattacharya and K.P. Ghatak, *Effective Electron Mass in Low-Dimensional Semiconductors*, Springer (2013).

[6] I. Crassee, J. Levallois, A.L. Walter, M. Ostler, A. Bostwick, E. Rotenberg, T. Seyller, D. van der Marel and A.B. Kuzmenko, Nature Physics **7**, 48 (2011).

[7] L. Wu, W-K. Tse, M. Brahlek, C.M. Morris, R.V Aguilar, N. Koirala, S. Oh and N.P. Armitage, Physical Review Letters **115**, 217602 (2015).

[8] S.V. Dordevic, G.M. Foster, M.S. Wolf, N. Stojilovic, H. Lei, C. Petrovic, Z. Chen, Z.Q. Li and L.C. Tung, J.Phys.: Condens. Matter, **28**, 165602 (2016).

[9] J. Levallois, P. Chudzinski, J.N. Hancock, A.B. Kuzmenko and D. van der Marel, Phys.Rev.B **89**, 155123 (2014).

[10] P.J. de Visser, J. Levallois, M.K. Tran, J.-M. Poumirol, I.O. Nedoliuk, J. Teyssier, C. Uher, D. van der Marel and A.B. Kuzmenko, Phys.Rev.Lett. **117**, 017402 (2016).

[11] A. Koncz, A.D. LaForge, Z Li, A. Frenzel, B. Pursley, T. Lin, X. Liu, J. Shi, S.V. Dordevic and D.N. Basov 2010 *http://meetings.aps.org/link/BAPS.2010.MAR.H15.4*

[12] A.A. Schafgans, K.W. Post, A.A. Taskin, Y. Ando, X.-L. Qi, B.C. Chapler and D.N. Basov, Phys.Rev.B **85**, 195440 (2012).

[13] S.V. Dordevic, M.S. Wolf, N. Stojilovic, M.V. Nikolic, S.S. Vujatovic, P.M. Nikolic and L.C. Tung, Phys.Rev.B, **86**, 115119 (2012).

[14] S.V. Dordevic, G.M. Foster, N. Stojilovic, E.A. Evans, Z.G. Chen ,Z.Q. Li, M.V. Nikolic, Z.Z. Djuric, S.S. Vujatovic and P.M. Nikolic, Phys. Status Solidi B **251**, 1510 (2014).

[15] Y. Shao, K.W. Post, J.-S. Wu, S. Dai, A.J. Frenzel, A.R. Richardella, J.S. Lee, N. Samarth, M.M. Fogler, A.V. Balatsky, D.E. Kharzeev and D.N. Basov, Nano Letters **17**, 980 (2017).

[16] L.-C. Tung, W. Yu, P. Cadden-Zimansky, I. Miotkowski, Y.P. Chen, D. Smirnov and Z. Jiang Physical Review B **93**, 085140 (2016).

[17] Z. Fisk and J.P. Remeika, *Handbook on the Physics and Chemistry of Rare Earths*, edited by Gschneider K A and Eyring J (Amsterdam:Elsevier), Vol. 12 (1989).

[18] C.P. Canfield and Z. Fisk, Philosophical Magazine B **65**, 1117 (1992).

[19] B. Hunter, *Rietica - A visual Rietveld program*, International Union of Crystallography Commission on Powder Diffraction Newsletter No. 20, (Summer) http://www.rietica.org (1998).

[20] S.V. Dordevic, M.S. Wolf, N. Stojilovic, H. Lei and C Petrovic, J.Phys.: Condens. Matter, **25**, 075501 (2013).

[21] A cyclotron resonance was obsreved in a recent magneto-transmission study of Bi_2Te_3 nano-flakes[16].

[22] B. Lax and J.G. Mavroides, *Semiconductors and Semimetals*, edited by R.K. Willardson and A.C. Beer, Academic Press, New York and London (1967).

[23] A.D. LaForge, A. Frenzel, B.C. Pursley, T. Lin, X. Liu, J. Shi and D.N. Basov, Physical Review B **81**, 125120 (2010).

[24] M.P. Marder, *Condensed Matter Physics*, Wiley (2000).

[25] H. Kohler, Physica Status Solidi B **74**, 591 (1976).

[26] V.A. Kulbachinskii, N. Miura, H. Nakagawa, H. Arimoto, T. Ikaida, P. Lostak and C. Drasar, Phys.Rev.B **59**, 15733 (1999).

[27] R.A. Davison, L.V. Delacretaz, B. Gouteraux and S.A. Hartnoll, Phys.Rev.B **94**, 054502 (2016).

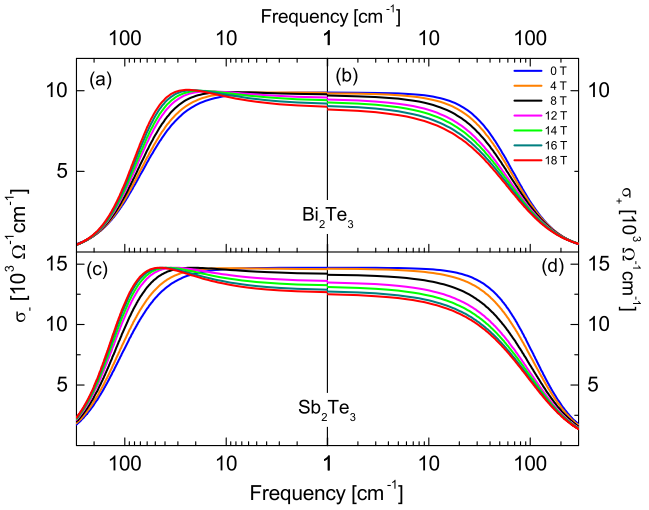

FIG. 3: (Color online). (a) and (b) Optical conductivities for left and right circularly polarized light $\sigma_+(\omega)$ (right panel) and $\sigma_-(\omega)$ (left panel) for Bi_2Te_3 at different magnetic fields, generated from the best fits of reflection ratios (Fig. 2). (c) and (d) Optical conductivities $\sigma_+(\omega)$ and $\sigma_-(\omega)$ for Sb_2Te_3. The same color coding is used in all four panels.

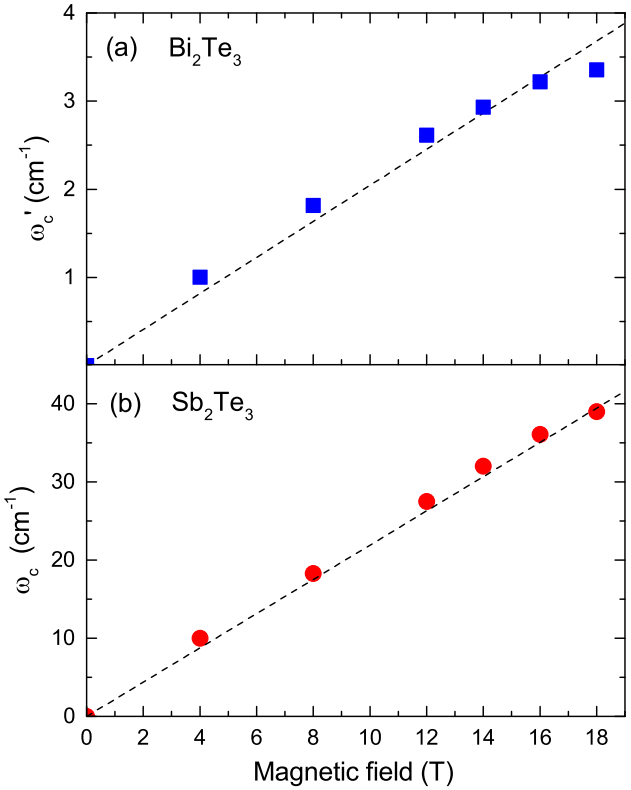

FIG. 4: (Color online). (a) Magnetic field dependence of cyclotron frequency $\omega_c^{'}$ in Bi_2Te_3. Dashed line is a linear fit of the data. (b) Cyclotron resonance frequency ω_c of Sb_2Te_3. Dashed line is a linear fit, from which the cyclotron effective mass of 0.42 m_e was extracted.